



**Synthesis of Gold and Silver Nanoparticles and
Characterization of Structural, Optical,
and Electronic Properties**

by Eric N. Lee, Mark H. Griep, and Shashi P. Karna

ARL-TR-5763

September 2011

NOTICES

Disclaimers

The findings in this report are not to be construed as an official Department of the Army position unless so designated by other authorized documents.

Citation of manufacturer's or trade names does not constitute an official endorsement or approval of the use thereof.

Destroy this report when it is no longer needed. Do not return it to the originator.

Army Research Laboratory

Aberdeen Proving Ground, MD 21005-5069

ARL-TR-5763

September 2011

Synthesis of Gold and Silver Nanoparticles and Characterization of Structural, Optical, and Electronic Properties

Eric N. Lee

University of Maryland, College Park

Mark H. Griep and Shashi P. Karna

Weapons and Materials Research Directorate, ARL

REPORT DOCUMENTATION PAGE			Form Approved OMB No. 0704-0188		
Public reporting burden for this collection of information is estimated to average 1 hour per response, including the time for reviewing instructions, searching existing data sources, gathering and maintaining the data needed, and completing and reviewing the collection information. Send comments regarding this burden estimate or any other aspect of this collection of information, including suggestions for reducing the burden, to Department of Defense, Washington Headquarters Services, Directorate for Information Operations and Reports (0704-0188), 1215 Jefferson Davis Highway, Suite 1204, Arlington, VA 22202-4302. Respondents should be aware that notwithstanding any other provision of law, no person shall be subject to any penalty for failing to comply with a collection of information if it does not display a currently valid OMB control number. PLEASE DO NOT RETURN YOUR FORM TO THE ABOVE ADDRESS.					
1. REPORT DATE (DD-MM-YYYY) September 2011		2. REPORT TYPE Final		3. DATES COVERED (From - To) September 2009–August 2010	
4. TITLE AND SUBTITLE Synthesis of Gold and Silver Nanoparticles and Characterization of Structural, Optical, and Electronic Properties			5a. CONTRACT NUMBER		
			5b. GRANT NUMBER		
			5c. PROGRAM ELEMENT NUMBER		
6. AUTHOR(S) Eric N. Lee,* Mark H. Griep, and Shashi P. Karna			5d. PROJECT NUMBER 622618		
			5e. TASK NUMBER		
			5f. WORK UNIT NUMBER		
7. PERFORMING ORGANIZATION NAME(S) AND ADDRESS(ES) U.S. Army Research Laboratory ATTN: RDRL-WMM-A Aberdeen Proving Ground, MD 21005-5069			8. PERFORMING ORGANIZATION REPORT NUMBER ARL-TR-5763		
9. SPONSORING/MONITORING AGENCY NAME(S) AND ADDRESS(ES)			10. SPONSOR/MONITOR'S ACRONYM(S)		
			11. SPONSOR/MONITOR'S REPORT NUMBER(S)		
12. DISTRIBUTION/AVAILABILITY STATEMENT Approved for public release; distribution is unlimited.					
13. SUPPLEMENTARY NOTES *University of Maryland, College Park, MD 20742					
14. ABSTRACT Metallic nanoparticles, most notably gold and silver, portray multiple structural, optical, electronic, and photoelectric properties, all of which often vary with particle diameter. When synthesized as alloys, as compared to purely monometallic particles, changes in the synthesis procedure and conditions can yield entirely unique particles with variable absorbance levels, sizes, and emission intensities, and stronger characteristics much more suited for use in electronic applications. Through solution-phase synthesis and replacement-reaction synthesis, this experiment generated both single element nanoparticles within the quantum range (<15 nm in diameter) and alloy nanoparticles of gold and silver in aqueous solution. Through ultraviolet-visible spectroscopy and spectrofluoroscropy, the existence of an alloy metal was characterized through the presence of a single combined absorbance and emission peak. Particle size analysis through dynamic light scattering, atomic force microscopy, and transmission electron microscopy concluded that alloy nanoparticles synthesized through replacement reactions resulted in an even size distribution of particles. These characteristics combined with the ability to modify particle size and resulting characteristics make this method of synthesis much more useful in a wide array of applications.					
15. SUBJECT TERMS nanoparticles, alloy, TEM, Au, Ag, AFM, UV-Vis, QD					
16. SECURITY CLASSIFICATION OF:			17. LIMITATION OF ABSTRACT UU	18. NUMBER OF PAGES 22	19a. NAME OF RESPONSIBLE PERSON Mark Griep
a. REPORT Unclassified	b. ABSTRACT Unclassified	c. THIS PAGE Unclassified			19b. TELEPHONE NUMBER (Include area code) 410-306-4953

Contents

List of Figures	iv
1. Introduction and Background	1
2. Materials and Experimental Procedure	2
3. Results and Discussion	3
3.1 Absorbance and Emission Spectra	3
3.2 Atomic Force Microscopy Analysis.....	6
3.3 Transmission Electron Microscopy Analysis.....	8
4. Summary and Final Conclusions	9
5. References	11
List of Symbols, Abbreviations, and Acronyms	13
Distribution List	14

List of Figures

Figure 1. UV-Vis absorption spectra of pure Au NP, pure Ag NP, and varying mixtures of alloy Au-Ag NPs, each with varying absorbance peaks.	4
Figure 2. Emission spectra of pure Au NPs and pure Ag NPs. Each monometallic sample has a single excitation wavelength, which results in a single emission peak.	5
Figure 3. Emission spectra of alloy Au-Ag NPs (excitation at 300 nm). Emission corresponding to Ag energy spectrum.	5
Figure 4. Emission spectra of alloy Au-Ag NPs (excitation at 510 nm). Emission corresponding to Au energy spectrum.	6
Figure 5. Noncontact mode AFM image of Au-Ag alloy NPs. Image shows 3-D topography of samples in a 4×4 - μm scan. Particles are evenly distributed among the scan area.	6
Figure 6. Noncontact mode AFM images of Au-Ag alloy NPs. Image shows 2-D scan of samples at a scan size of $4 \times 4 \mu\text{m}$. Particles have formed evenly throughout the solution and with slightly varying diameter.	7
Figure 7. Height profile of large Au-Ag alloy particle as scanned by AFM. Particle radius as measured along the z-axis was 4.207 nm.	7
Figure 8. Height profile of average Au-Ag alloy particle as scanned by AFM. Particle radius as measured along the z-axis was 1.969 nm.	8
Figure 9. High-resolution TEM images of alloy gold and silver QDs at various scan sizes: (a) 20 nm (partially formed NPs on the edge of the circular pattern), (b) 50 nm (sample forms in random patterns as particle aggregate), (c) 5 nm (sample forms in small groups), and (d) 200 nm (samples form in semi-circular constructs).	9

1. Introduction and Background

Quantum dots (QDs) are microscopic particles or atomic clusters measured on the nanometer scale (10^{-9} m), and they hold many optical, electronic, structural, and photoelectric properties that make them useful in a variety of practical applications in various fields, from photovoltaic cells to light-emitting diodes. Studies have shown that nanoparticles (NPs) can yield high quantum yield, colloidal stability, and conjugation with biomolecules, making them useful in a wide array of engineered applications (1). One major characteristic of QDs is their size-dependent properties, whose emission and absorption levels can be adjusted by finely tuning their size on the nanometer scale. Due to their relative sensitivity to particle size, methods for synthesizing QDs with modifiable diameters are essential, as their resulting optical properties directly correlate with their physical dimensions. The ability to generate microscopic particles that can perform a wide variety of tasks makes QDs ideal in creating small and cost-efficient electronic devices. Through structural and spectroscopic analysis, this work will test the various properties of gold and silver QDs engineered toward bionanomaterial applications.

A wide range of possible methodologies used to generate QDs are available, each resulting in a variety of sizes and final products. QDs can also be generated on all types of substrates and hosts, often silicon-based (2–6). Each method had different effects on final QD characteristics (7). One method involves creating a silica host with microscopic pore diameters and submerging the host in chloroauric acid (HAuCl_4), filling the pores with metal NPs (8). This method slightly affected the optical and luminescent properties of the QDs. Other methods synthesize gold nanoclusters by dissolving chloroauric acid in an aqueous PAMAM (poly[amidoamine] dendrimer, or synthetic polymers with repeating monomer units of $\text{CH}_2 - \text{CH}_2 - \text{CO} - \text{NH} - \text{CH}_2 - \text{CH}_2 - \text{N}$) solution and adding sodium borohydride (NaBH_4), which reduces gold ions. This method generates differently sized fluorescent gold nanoclusters that exhibit discrete excitation and emission spectra from the ultraviolet (UV) to the near infrared (IR). Each change in luminescence corresponded with a different peak during spectrum analysis (UV corresponded with Au_5 , IR with Au_{31} , etc.) (9). Methods even exist to synthesize alloy NPs using ingredients found in nature (10).

However, the methods used in this study involve solution-phase and replacement reaction synthesis. This method of generating gold and silver alloy NPs is ideal for analytical purposes because of the ease of size modification. Gold-silver (Au-Ag) alloy NPs can be synthesized by reducing chloroauric acid and silver nitrate (AgNO_3) with sodium borohydride and sodium citrate (11). The size of the particles synthesized could be increased or decreased using various initial gold-to-silver molar ratios, and the resulting size distributions could be studied in a variety of ways (12). The correlation between molar ratio and luminescent and optical properties was explored, and the study found that a general increase in the fraction of silver to gold moles

resulted in an increased maximum wavelength. This relationship followed the model $N^{1/3}$, also known as a jellium model, with N being the number of atoms in a cluster (11). As many characteristics of QDs rely on particle diameter, it is important to discover a possible correlation between fluorescence, emissions, wavelength, and particle size.

The optical properties of each sample also play a major role (13, 14). Spectrometers can be used to analyze the absorption spectra of resultant QDs, even in aqueous solution. These spectra show where each sample best absorbs light—an important characteristic in energy conversion (14). Spectrofluorometers also return a spectrum but instead show where the sample emits its absorbed energy when excited at another wavelength. These luminescent qualities are important when using QDs in other applications (15). Fine-tuning these variables and learning how they correlate with size are critical steps to creating electronics out of QDs. Previous work has shown a possible relationship between the amounts and sizes of gold and silver shells in alloy NPs and optical properties (16). Studies have been performed on the correlation between emission energy and monometallic quantum dot clusters, but less work has been performed on alloy samples (17). Previous studies have shown that in monometallic gold samples, smaller cluster sizes resulted in higher emission energy, but it is unclear whether this carries over into alloy samples as well (18).

While many studies have researched the various characteristics of monometallic quantum dots and their optical, structural, and electronic properties, further progress is needed when working with alloy Au-Ag QDs. Both types of NPs have the potential to create efficient electronic devices, including light-emitting diodes and solar cells (19). Much research has gone into improving the efficiency of QD devices, and the introduction of alloys could further this effort (20, 21). Alloy QDs have already shown great merit in biological applications, such as sensors and markers that are biologically stable in other organisms (1, 22). By finding correlations between particle size and optical characteristics, researchers may discover a method for synthesizing particles with fine-tunable properties for multiple applications.

2. Materials and Experimental Procedure

Pure gold and silver QDs were created via solution-phase synthesis, which was performed by combining 100 mL of filtered 18.1-M Ω distilled water and 50- μ L 0.01-M sodium citrate. A total of 50 μ L consisting of a combination of 0.01-M AgNO₃ and 0.01-M HAuCl₄ was then added. The solution was prepared in 125-mL Pyrex glass beakers with magnetic stir bars and was lightly stirred for 1 min. A total of 50 μ L of 0.01-M sodium borohydride, chilled prior to the experiment, was then added to the solution, and the beaker was vigorously stirred for 3 min. Prepared solutions were then wrapped and stored in a dark area pending analysis.

Alloy NP synthesis via replacement reaction was performed in similar 125-mL Pyrex glass beakers with magnetic stir bars. Six beakers were filled with 5 mL of 20-mM AgNO_3 and 5 mL of 0.2 M, 10,000 molar weight polyvinylpyrrolidone (PVP). PVP, a synthetic polymer, is used to encase and protect the pure Ag NPs. In addition, 2 mL of 20-mM potassium hydroxide in pellet form and 83 mL of distilled water were added. The solution was stirred for 30 min. Then, 5 mL of 0.1-M NaBH_4 , chilled prior to the experiment, was quickly injected into the solution. The solution was allowed to stir for 1 h to complete the reaction, and the solution was finally wrapped and stored for 48 h in order to allow the residual NaBH_4 to precipitate. Afterward, 20 mL of the solution was poured into beakers and heated to 100 °C. Varying amounts of 1-mM HAuCl_4 were then added under heat, which ranged from 3 to 5 mL, and were stirred and heated for 10 min. The solutions were cooled and precipitated for 24 h and then finally stored in a dark area pending analysis.

Ultraviolet-visible (UV-Vis) spectroscopy for sample absorbance characteristics was performed on a CCD Array Spectrophotometer. Distilled water was used as a blank, and absorbance levels were collected on high precision. Spectrofluorometry and emission level collection was performed using a spectrofluorometer. Atomic force microscopy was performed in non-contact mode. Detailed particle size was analyzed with a Dynamic Light Scattering Particle Size Analyzer and a transmission electron microscope.

3. Results and Discussion

3.1 Absorbance and Emission Spectra

After synthesis of both monometallic and alloy NPs, UV-Vis spectroscopy was performed on the samples. Scans were run in the visible spectrum (375–775 nm), and spectra were zeroed at 775 nm. The absorbance spectrum, as shown in figure 1, displays a direct correlation with the amount of chloroauric acid (gold) and the absorbance peak of the sample. Pure silver NPs demonstrated an absorbance of violet light with a maxima at 413 nm, while pure gold NPs demonstrated an absorbance of green light with a maxima at 530 nm. The three alloy samples displayed much more unique optical properties. Two out of the three alloy samples had broad ranges of absorbance instead of single peaks. As seen in figure 1, the alloy samples synthesized with 3 and 4 mL of chloroauric acid absorbed energy between 375 and 508 nm. The alloy sample synthesized with 5 mL of chloroauric matched that of pure gold NPs. In general, as the amount of chloroauric acid added to the solution increased, the absorbance peak shifted to the right, closer to the pure gold spectrum and closer to the red portion of the visible spectrum. As seen with the 5-mL sample, adding too much gold during the synthesis process causes silver's optical characteristics to disappear from the absorbance spectra altogether.

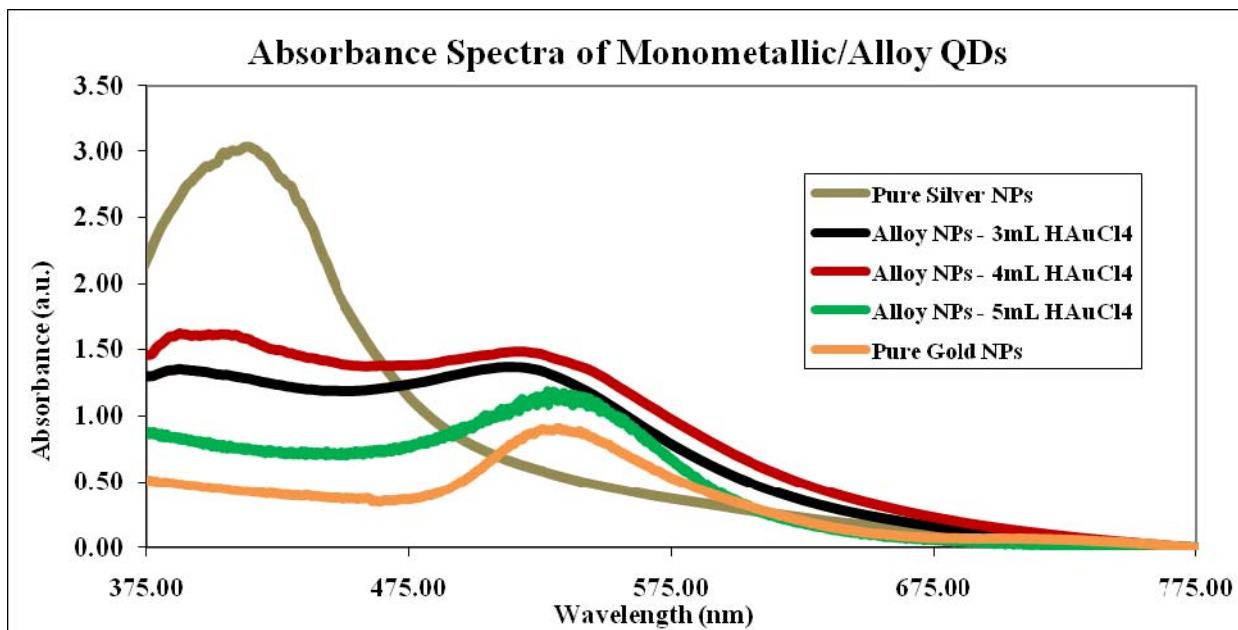


Figure 1. UV-Vis absorption spectra of pure Au NP, pure Ag NP, and varying mixtures of alloy Au-Ag NPs, each with varying absorbance peaks.

Emission scans were ran using the spectrofluorometer’s built-in “discover” scan, which tested multiple excitation wavelengths and checked each for actual energy emissions. These scans found that the monometallic samples displayed a single excitation peak and therefore one emission peak. For the alloy samples, the scan found two excitation peaks and two corresponding emission peaks. Emission intensity spectra are shown in figures 2–4. Figure 2 shows emission spectra for monometallic Au samples, and figures 3 and 4 show emission spectra for the alloy samples. When pure gold and alloy samples were excited with green light (495–570 nm), both samples were seen to emit red light at 658 nm. When pure silver samples were excited with violet light (410 nm), they emitted violet light as well, at around 364 nm. Additionally, alloy samples were seen to have a second excitation/emission peak. When excited at UV wavelengths (10–400 nm), alloy samples would emit violet light at a peak wavelength of 435 nm.

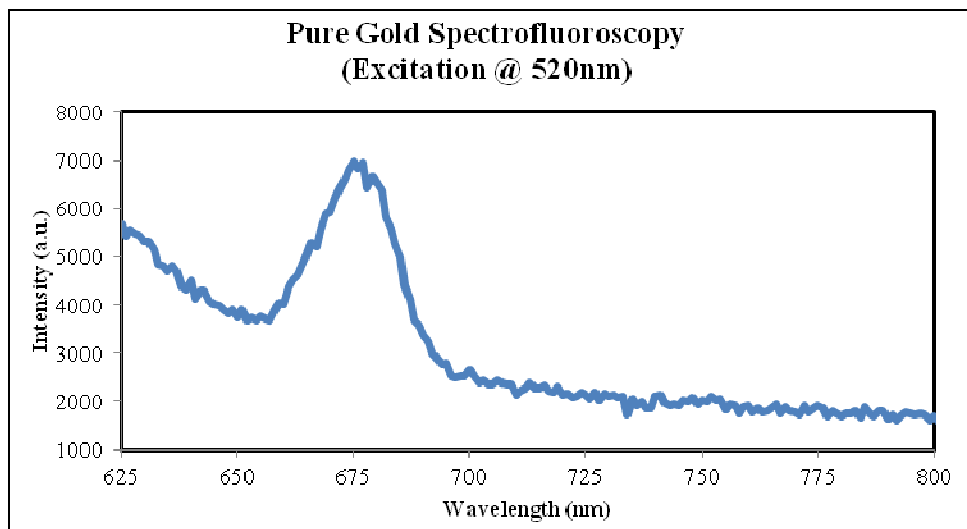


Figure 2. Emission spectra of pure Au NPs and pure Ag NPs. Each monometallic sample has a single excitation wavelength, which results in a single emission peak.

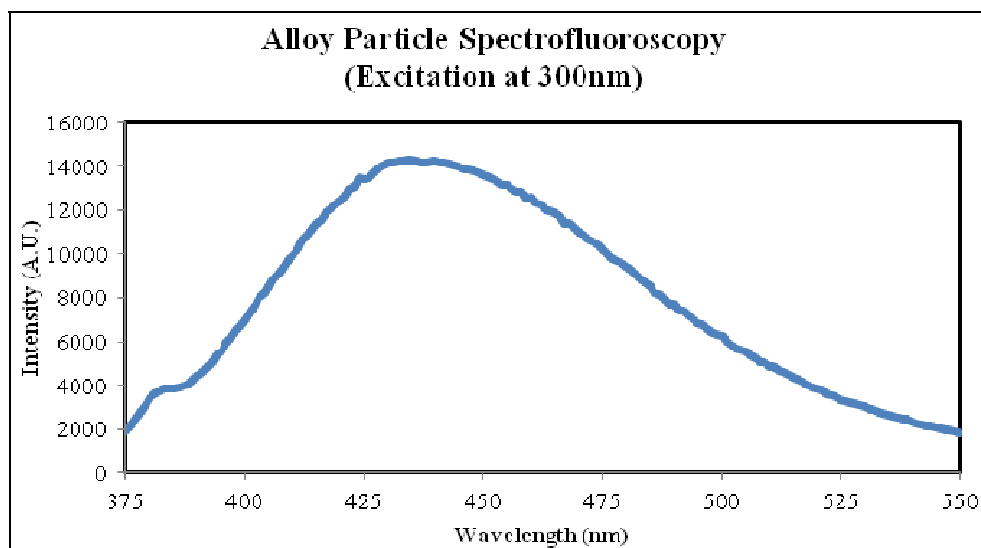


Figure 3. Emission spectra of alloy Au-Ag NPs (excitation at 300 nm). Emission corresponding to Ag energy spectrum.

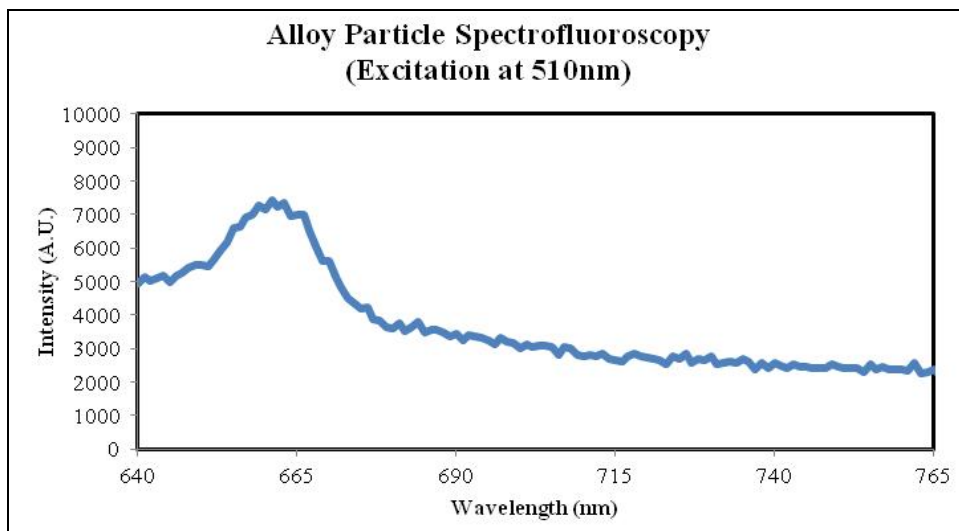


Figure 4. Emission spectra of alloy Au-Ag NPs (excitation at 510 nm). Emission corresponding to Au energy spectrum.

3.2 Atomic Force Microscopy Analysis

Atomic force microscopy (AFM) was performed on alloy Au-Ag samples to check for the presence of particles, the preliminary particle size, and the overall size distribution. AFM was performed in noncontact mode, and images were returned in two forms: three-dimensional (3-D) topography and two-dimensional (2-D) scans.

Alloy sample AFM images concluded the presence of NPs, as shown in figures 5 and 6. When measuring via the z-axis, the particle size matched data returned via transmission electron microscopy (TEM) imagery. The particle diameter was measured to be around 3 nm, as shown in figures 7 and 8. Particles were evenly distributed throughout the sample, and a large amount of particles appeared on a $4\text{-}\mu\text{m} \times 4\text{-}\mu\text{m}$ scan.

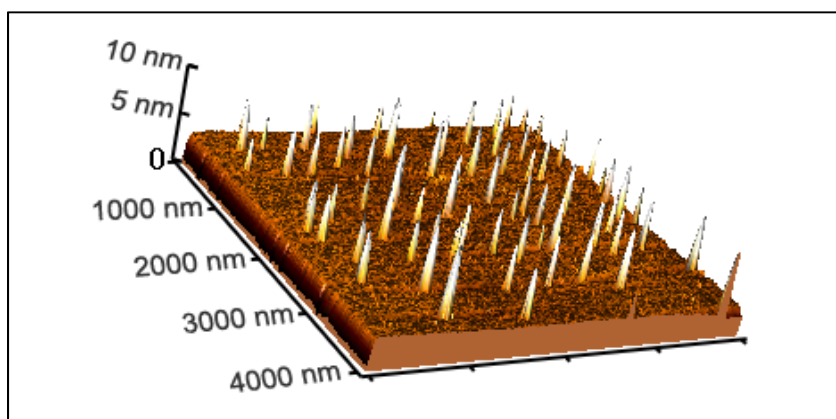


Figure 5. Noncontact mode AFM image of Au-Ag alloy NPs. Image shows 3-D topography of samples in a $4\text{-}\mu\text{m} \times 4\text{-}\mu\text{m}$ scan. Particles are evenly distributed among the scan area.

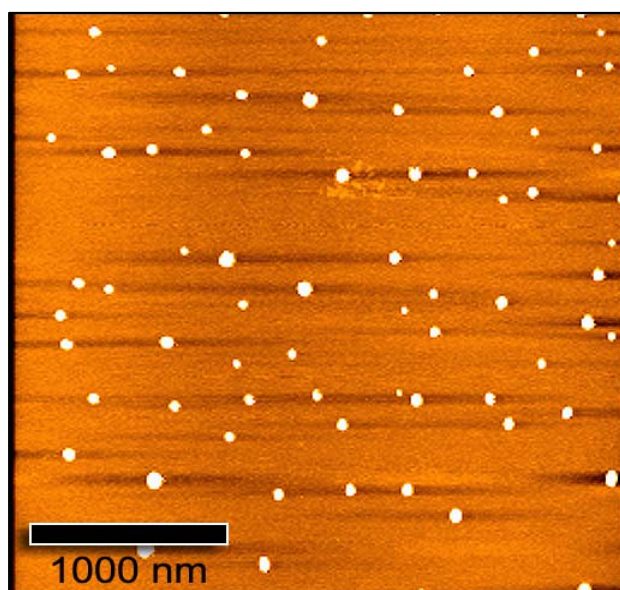


Figure 6. Noncontact mode AFM images of Au-Ag alloy NPs. Image shows 2-D scan of samples at a scan size of $4 \times 4 \mu\text{m}$. Particles have formed evenly throughout the solution and with slightly varying diameter.

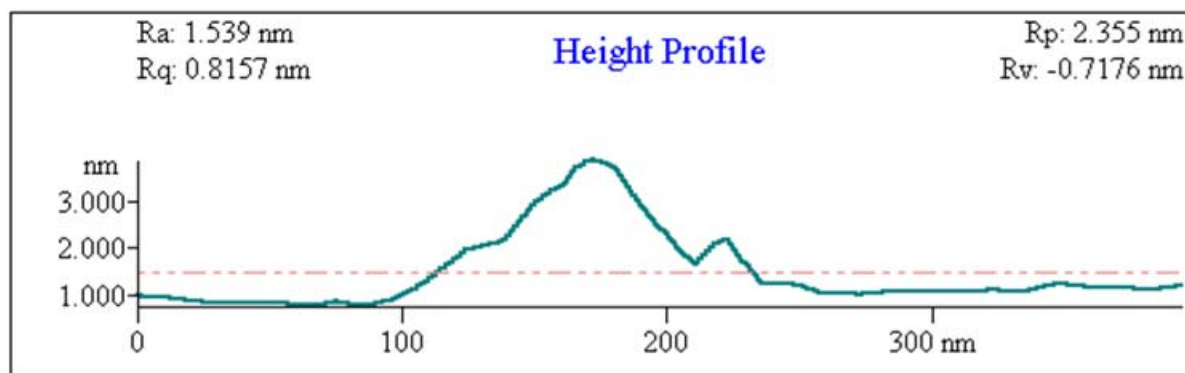


Figure 7. Height profile of large Au-Ag alloy particle as scanned by AFM. Particle radius as measured along the z-axis was 4.207 nm.

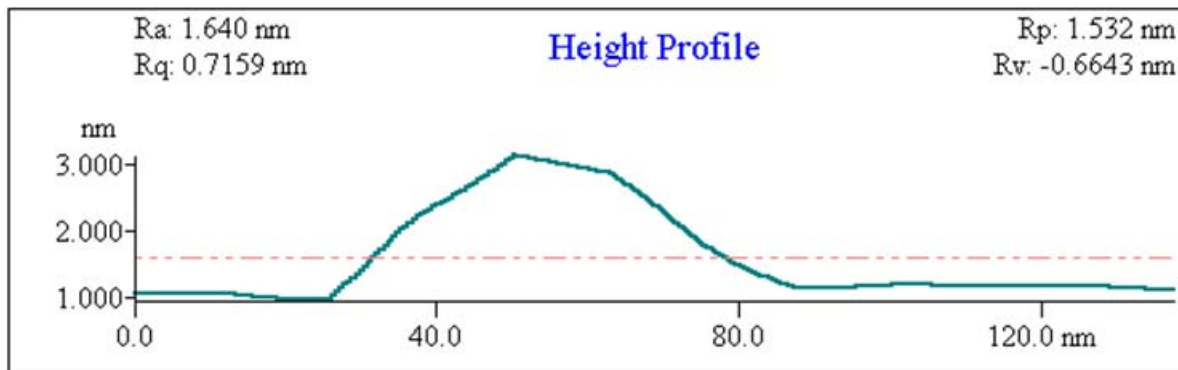


Figure 8. Height profile of average Au-Ag alloy particle as scanned by AFM. Particle radius as measured along the z-axis was 1.969 nm.

3.3 Transmission Electron Microscopy Analysis

TEM was also used as a primary method to determine physical characteristics. Image scans were run at varying scan sizes, as shown in figure 9 (a–d), from 200 to 3000 nm. The resulting images confirm the synthesis of alloy gold and silver NPs. The images also conclude that particles formed with a fairly even size distribution. Many of the particles fell within the sub-10-nm range. While atomic force microscopy concluded that some particles were large and outside of the quantum dot range, samples scanned via TEM had an average particle diameter that fell within the quantum dot range (<15 nm). Alloy samples demonstrated average diameters between 5 and 6 nm, and monometallic gold and silver samples with 9.40 and 12.1 nm, respectively. Alloy samples form in circular patterns. Some particle aggregation, which may have occurred over time, was present in the samples. Images show that the NPs often aggregate into circular or semi-circular patterns. Traces of undeveloped NPs lie inside of these semi-circular constructs, as shown in figure 9. Larger particles seem to move toward the exterior of the circle, while newer particles are seen to form along the interior of the circle. A longer boiling period during the synthesis method may allow a larger number of particles to form.

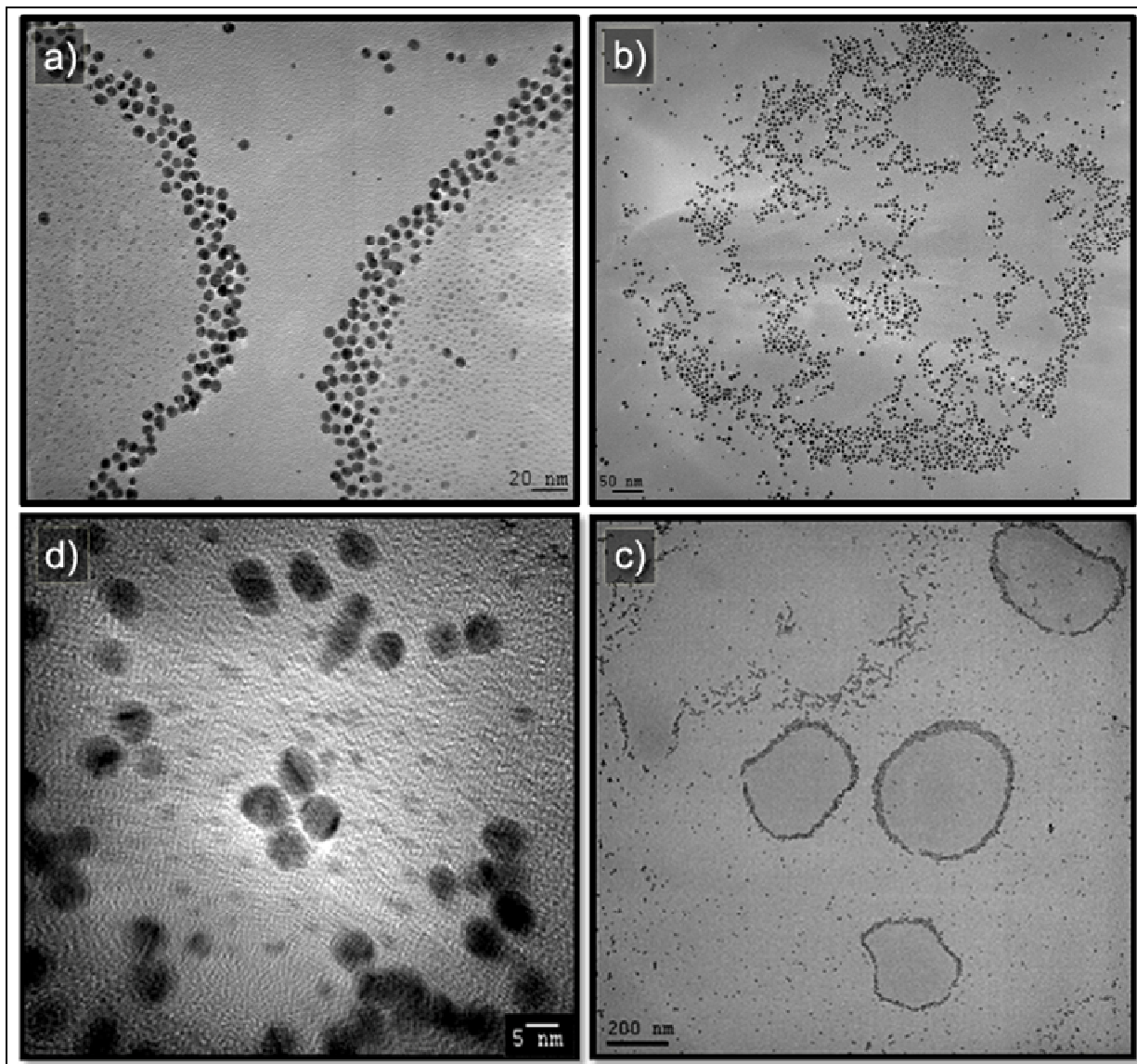


Figure 9. High-resolution TEM images of alloy gold and silver QDs at various scan sizes: (a) 20 nm (partially formed NPs on the edge of the circular pattern), (b) 50 nm (sample forms in random patterns as particle aggregate), (c) 5 nm (sample forms in small groups), and (d) 200 nm (samples form in semi-circular constructs).

4. Summary and Final Conclusions

Through replacement reactions and solution-phase reactions, both alloy gold and silver NPs and monometallic particles were successfully synthesized. Silver nitrate and sodium borohydride were combined and precipitated to create silver NPs, and chloroauric acid was then added under heat to alloy the sample with gold NPs. After synthesis, structural, optical, and electronic characteristics of the samples were analyzed. AFM, TEM, UV-Vis, and fluoroscopy were used

to determine average particle diameter, absorbance peaks, emission peaks, and size distribution. Both the monometallic and alloy samples fell within the necessary size requirement for quantum dots when analyzed under TEM. Samples also exhibited an even size distribution and formed semi-circular patterns.

In terms of optical characteristics, alloy samples displayed absorbance and emission spectra unique to those of pure monometallic samples. Alloy samples had a much broader absorbance peak, which varied depending on the amount of chloroauric acid used in the synthesis method. Increasing the amount of chloroauric acid, in general, shifted the absorbance peak toward the red portion of the visible spectrum (620 nm). Optical characteristics also confirmed the creation of an alloy solution, as opposed to a mixture, due to the presence of a unified absorption peak.

The emission spectra of these alloy samples have shown that these NPs hold greater potential for use in applied devices, such as solar cells, because of two emission peaks. This means that they absorb energy and become excited at two different wavelengths for energy emission, which could prove useful in electronic applications. Mixtures of multiple types and sizes of alloy quantum dots could serve to absorb and emit energy on a wide range of wavelengths and therefore increase electronic efficiency.

Synthesis and characterization of alloy quantum dots show that the resultant sample could yield characteristics entirely unique from the source elements. In this scenario, an alloy between gold and silver NPs yielded dual emission spectra and ease of optical modifications, which could be useful in a variety of electronic applications.

5. References

1. Lin, C. J.; Yang, T.; Lee, C.; Huang, S.; Sperling, R.; Zanella, M.; Li, J.; Shen, J.; Wang, H.; Yeh, H.; Parak, W.; Chang, W. Synthesis, Characterization, and Bioconjugation of Fluorescent Gold Nanoclusters Toward Biological Labeling Applications. *American Chemical Society* **2009**, *3*, 395–401.
2. Zhang, H.; Jin, C.; Mirkin, A. Synthesis of Open-Ended, Cylindrical Au-Ag Alloy Nanostructures on a Si/SiOX Surface. *Nano Letters* **2004**, *4*, 1493–1495.
3. Zhou, M.; Chen, S.; Zhao, S.; Ma, H. One-Step Synthesis of Au-Ag alloy Nanoparticles by a Convenient Electrochemical Method. *Physics E* **2006**, *33*, 28–34.
4. Pal, A.; Shah, S.; Devi, S. Synthesis of Au, Ag and Au-Ag Alloy Nanoparticles in Aqueous Polymer Solution. *Colloids & Surfaces A: Phys. Eng* **2007**, *302*, 51–57.
5. Mondal, S.; Roy, N.; Laskar, R. A.; Sk, I.; Basu, S.; Mandal, D.; Begum, N. A. Biogenic Synthesis of Ag, Au and Bimetallic Au/Ag Alloy Nanoparticles Using Aqueous Extract of Mahogany. *Colloids & Surfaces B: Biointerfaces* **2011**, *82*, 497–504.
6. Yin, Y.; Alivisatos, A. Colloidal Nanocrystal Synthesis and the Organic–Inorganic Interface. *Nature* **2005**, *437*, 664–670.
7. Chen, W.; Chi, W.; Zhang, L.; Wang, G.; Zhang, L. Sonochemical Processes and Formation of Gold Nanoparticles Within Pores of Mesoporous Silica. *Journal of Colloid and Interface Science* **2001**, *238*, 1609.
8. Zheng, J.; Petty, J.; Dickson, R.; High Quantum Yield Blue Emission From Water-Soluble Au₈ Nanodots. *American Chemical Society* **2003**, *125*, 7780–7781.
9. Okazaki, K.; Kiyama, T.; Hirahara, K.; Tanaka, N.; Kuwabata, S.; Torimoto, T. Single-Step Synthesis of Gold–Silver Alloy Nanoparticles in Ionic Liquids by a Sputter Deposition Technique. *Chemical Communications* **2008**, *6*, 691–693.
10. Mallin, M.; Murphy, C. Solution-Phase Synthesis of Sub-10 nm Au–Ag Alloy Nanoparticles. *American Chemical Society, Nano Letters* **2002**, *2*, 1235–1237.
11. Liu, H.; Huang, L.; Zhu, J. Tunable Intrinsic Optical Bistability of Au–Ag Alloy Nanoparticle: Effects of Spatial Position and Au Composition. *European Physical Journal B – Condensed Matter* **2010**, *77*, 133–137.
12. Wilcoxon, J., Martin, J., Provencio, P. Size Distributions of Gold Nanoclusters Studied by Liquid Chromatography. *Journal of Physical Chemistry B*. **2009**, *113*, 2647–2656.

13. Sun, Y.; Zhou, B.; Lin, Y.; Wang, W.; Shiral, F.; Pathak, P. Quantum-Sized Carbon Dots for Bright and Colorful Photoluminescence. *Journal of the American Chemical Society* **2006**, *128*, 7756–7757.
14. Chen, Y.; Rosenzweig, Z. Luminescent CdSe Quantum Dot Doped Stabilized Micelles. *American Chemical Society* **2002**, *2* (11), 1299–302.
15. Hubenthal, F.; Ziegler, T.; Hendrich, C. Tuning the Surface Plasmon Resonance by Preparation of Gold-Core/Silver-Shell and Alloy Nanoparticles. *European Physics Journal D* **2005**, *34*, 165–168.
16. Zheng, J.; Zheng, C.; Dickson, R. Highly Fluorescent, Water-Soluble, Size-Tunable Gold Quantum Dots. *The American Physical Society*, **2004**, *93*, 077402.
17. Liu, X.; Li, C.; Xu, J.; Lv, J.; Zhu, M.; Guo, Y. Surfactant-Free Synthesis and Functionalization of Highly Fluorescent Gold Quantum Dots. *American Chemical Society*, **2008**, *112*, 10778–10783
18. Hasobe, T.; Imahori, H. Photovoltaic Cells Using Composite Nanoclusters of Porphyrins and Fullerenes With Gold Nanoparticles. *Journal of the American Chemical Society* **2004**, *127*, 1216–1228.
19. Johnston, K. W.; Pattantyus-Abraham, A. G.; Clifford, J. P.; Myrskog, S. H.; MacNeil, D. D. Schottky-Quantum Dot Photovoltaics for Efficient Infrared Power Conversion. *American Institute of Physics Probes* **2008**, *151115*, 92–94.
20. Loef, R.; Houtepen, A. J.; Talgorn, E.; Schoonman, J.; Goossens, A. Study of Electronic Defects in CdSe Quantum Dots and Their Involvement in Quantum Dot Solar Cells. *American Chemical Society* **2009**, *9* (2), 856–859.
21. Zheng, D.; Hu, C.; Gan, T.; Dang, X.; Hu, S. Preparation and Application of a Novel Vanillin Sensor Based on Biosynthesis of Au–Ag Alloy Nanoparticles. *Sensors and Actuators B: Chemical* **2010**, *148*, 247–252.
22. Lie, N.; Prall, B.; Klimov, V. Hybrid Gold/Silica/Nanocrystal-Quantum-Dot Superstructures: Synthesis and Analysis of Semiconductor-Metal Interactions. *American Chemical Society* **2006**, *128*, 15632–15633.

List of Symbols, Abbreviations, and Acronyms

2-D	two dimensional
3-D	three dimensional
AFM	atomic force microscopy
Ag	silver
AgNO ₃	silver nitrate
Au	gold
HAuCl ₄	chloroauric acid
NaBH ₄	sodium borohydride
NP	nanoparticle
QD	quantum dot
TEM	transmission electron microscopy
UV	ultraviolet
Vis	visible

NO. OF
COPIES ORGANIZATION

1 DEFENSE TECHNICAL
(PDF INFORMATION CTR
only) DTIC OCA
8725 JOHN J KINGMAN RD
STE 0944
FORT BELVOIR VA 22060-6218

1 DIRECTOR
US ARMY RESEARCH LAB
IMNE ALC HRR
2800 POWDER MILL RD
ADELPHI MD 20783-1197

1 DIRECTOR
US ARMY RESEARCH LAB
RDRL CIO LL
2800 POWDER MILL RD
ADELPHI MD 20783-1197

1 DIRECTOR
US ARMY RESEARCH LAB
RDRL CIO MT
2800 POWDER MILL RD
ADELPHI MD 20783-1197

1 DIRECTOR
US ARMY RESEARCH LAB
RDRL D
2800 POWDER MILL RD
ADELPHI MD 20783-1197

NO. OF
COPIES ORGANIZATION

ABERDEEN PROVING GROUND

6 DIR USARL
RDRL WMM A
M GRIEP (1)
S KARNA (5)

INTENTIONALLY LEFT BLANK.